Real-time Thermographic Object Tracking of the Body Temperature of a Neonate

Rassels, Kianoush; French, Paddy

DOI
10.1109/SSI56489.2022.9901432

Publication date
2022

Document Version
Final published version

Published in
Proceedings of Smart Systems Integration, SSI 2022

Real-time Thermographic Object Tracking of the Body Temperature of a Neonate

Kianoush Rassels
BioMechanical Engineering
TU-Delft
Delft, The Netherlands
K.Rassel@tudelft.nl

Paddy French
Bioelectronics Research Group
TU-Delft
Delft, The Netherlands
P.J.French@tudelft.nl

***Abstract*—Neonates can show sudden rapid body movements when they are in pain, need care, or need to be fed. They can also be very quiet and immovable or move very slowly when they are asleep or being fed. Monitoring a neonate's body temperature for a long time provides physicians and nurses valuable information about the health condition of the baby. Thermographic technology is a remote and very safe way to measure an accurate neonate's body temperature to monitor his/her vital signs. However, the tracking of an elastic thermographic profile of a subject with a random and erratic movement in the short- and long-term is a challenging task. The combination of the real-time thermographic detection and tracking system provides a safe and more robust non-invasive method to measure the vital signs and monitor the physiological changes of the neonates over time. However, this method can also be used for other target age groups.**

Keywords—Thermographic object tracking; thermography technology; premature babies, incubator; infrared thermal imaging; neonates; tracking body temperature; temperature measurement.

I. Introduction

Neonates who are born before 37 weeks have underdeveloped organs like the skin, lungs, and a weak immune system, etc. making them weak and susceptible to diseases. For these reasons, premature babies do not have mechanisms to control their body temperature. Thus, they must be safeguarded in a conditioned and controlled environment against hypothermia or hyperthermia like an incubator.

During the first weeks and months after birth, the neonate's skin is quite fragile and needs time to develop until it reaches maturity [1]. By measuring and monitoring the vital signs and in particular the body temperature of a neonate for a long time, valuable information about the baby's health condition can be provided to the physicians and nurses. Using a traditional method like temperature sensors attached to a baby's body is not ideal or without risks if a neonate's body temperature needs to be measured and monitored many times. It could cause distress, irritation of the skin, and even result in an infection or hygienic concern for the baby [2],[3].

A remote real-time tracking and monitoring system like a thermal camera together with an embedded Single Board Computer (SBC) for the number crunching and pattern recognition provides a harmless and non-invasive solution. It can measure the global and local temperature of a Region of Interest (ROI) in the short- and long-term to have a better and more reliable non-invasive monitoring mechanism of the vital signs and physiological changes of the neonates.

Although real-time thermographic profile tracking is a challenging task [4], by monitoring the vital signs and following the variations and trends of the Thermal Profile Region (TPR), one can extract valuable physiological features and patterns with techniques like Artificial Intelligence, Machine Learning, or Deep Learning.

This paper discusses a real-time novel technique to (re-)track a single TPR for short- and long-term using a dedicated embedded system and software that provides non-invasive and more accurate information about a baby's health conditions for the carers.

II. Measurement Setup

The measurement setup consists of a thermal camera, a Single Board Computer (SBC), Linux operating system Lubuntu 20.04, and dedicated software running on the SBC for the pre- and post-processing of the thermal images.

A. Hardware and Software

In this research, a FLIR SC305 infrared camera connected to a Pine RockPro64 (SBC) has been used, see Fig. 1. The SBC specs are a Rockchip RK3399 Hexa-core System on Chip (SOC) as well as a quad-core Mali-T860MP4 with 4GB of dual-channel LPDDR4 system memory. The thermal measurements are done with a 9 Hz frame rate and a resolution of 320x240 pixels.

Fig. 1. FLIR SC305 infrared camera (left picture), Pine RockPro 64 (SBC) (right picture).

The infrared camera is connected via an ethernet cable to the SBC on which dedicated software is running to capture thermal images. In turn, these images are pre-processed to provide a thermal video stream in real-time. On each frame, each pixel is number crunched individually through the software with parameter settings such as temperature, humidity, emissivity, etc. to calculate the radiant energy emitted from the object in the form of the infrared wave. By compensating for the environmental variables and capturing infrared waves in the Field of View (FOV) of the thermal camera a very accurate temperature is calculated [5].

B. Measurement Setup

The environmental measurement for the thermal imaging can be modelled as depicted in Fig. 2. The temperature measurement can be done when the baby is outside an incubator (left picture) or when the baby is inside the incubator and the thermal camera is directed toward an open porthole (right picture).

2022 Smart Systems Integration (SSI) | 978-1-6654-8849-5/22/$31.00 ©2022 IEEE | DOI: 10.1109/SSI56489.2022.9901432

978-1-6654-8849-5/22/$31.00 ©2022 IEEE

In both cases, the radiation sources and thermal noise that can affect the temperature measurements are being compensated [5].

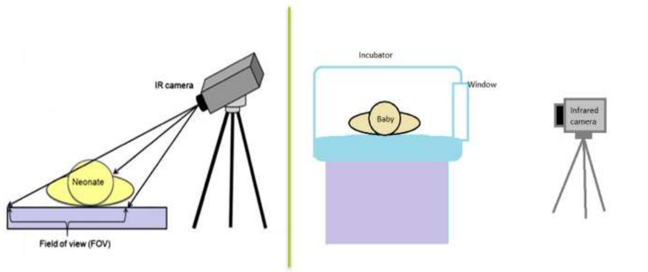

Fig. 2. Thermographic measurement model: The baby is out of the incubator (left picture), The baby is inside the incubator (right picture).

C. *Temperature Measurement*

For measuring the temperature in both thermographic models depicted in Fig. 2, the camera is positioned at some distance from the incubator so that it does not get in the way or interfere with carers' daily work. The lens of the Infrared camera is directed toward the neonate's body in such a way that the ROI in the FOV is within a 55º angle. This guarantees a constant directional emittance and reflectance during the temperature measurement [6]. Although, placing the camera in front of the opening (porthole) of the incubator satisfies this requirement because of the relatively small size of the porthole. In other words, in both thermographic measurement models depicted in Fig. 2, the FOV path of the infrared camera should completely be clear. It is because the incubator's Plexiglas hood is completely opaque to Infrared (IR).

III. Global and Local ROI Tracking and Used Techniques

This section provides a global overview of a real-time TPR detection and tracking system and sketches a fairly description of each step in the filter chain in Fig. 3.

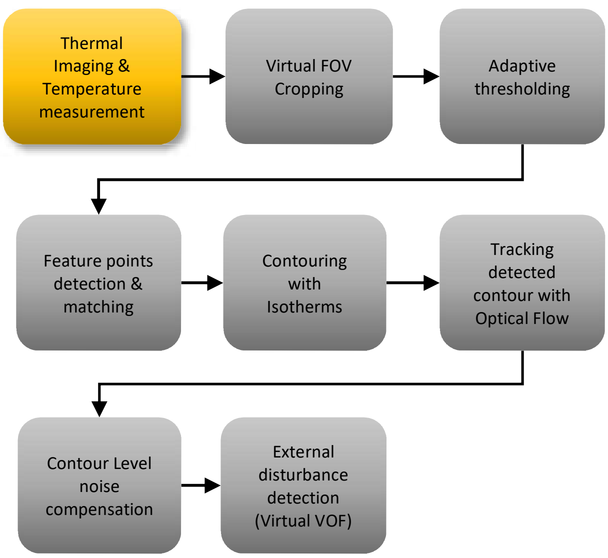

Fig. 3. Detecting and tracking filter chain of a Thermographic Profile Region.

A. *Thermal Imaging and Temperature Measurement*

From the pre-processed image frames captured by the thermal camera and after accurate temperature measurement, the global and local ROI is determined in real-time.

B. *Virtual Field of View Cropping*

Global ROI is the baby's temperature profile inside a user-defined frame called Virtual FOV, which is an enclosed bounding box. The local ROI is the TPR area with the highest body temperature of the baby in the Virtual FOV.

Tracking of a Thermal Profile Region (TPR) is achieved by tracking of local Region of Interest (ROI) supported by the global ROI considered as fine and coarse localization and tracking method, respectively. The local tracking is used for very small movements using a reference frame supported by the Optical Flow (OF). However, the latter is not able to redetect the lost TPR due to the neonate's displacement (disappearing of ROI from the camera's Field of View (FOV)) or rapid movement because of the limitations of the OF techniques. The lost ROI results in discarding the related consecutive frames. To solve this problem, long-term object tracking helps to redetect the lost TPR when it reappears in the thermal camera FOV, see Fig. 4.

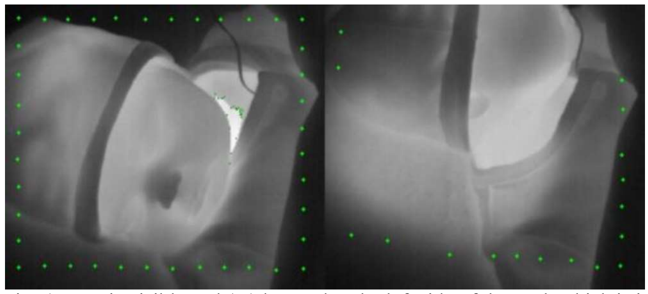

Fig. 4. TPR is visible and (re)detected at the left side of the neck which is in the FOV (left picture), TPR is lost because of the baby's head movement (right picture).

The feature tracking and triangulation techniques will help to predict the new location of the local ROI and recreate it by overlapping the new ROI with the ROI of the reference frame. If the overlapped region is more than 50% match with the original ROI, it is considered to be the valid recovered local ROI. Otherwise, the lost TPR is not retrievable, and an alarm will be sent to the nurse or physician providing care at that moment.

C. *Adaptive Thresholding*

Adaptive thresholding calculates the threshold value for each region in the frame [7]. This method can isolate distinct objects using different grey-scale values scattered across the frame even if they are contrasting with the local background, see Fig. 5.

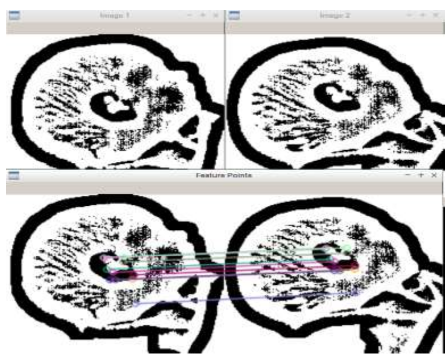

Fig. 5. Adaptive thresholding and feature point matching between 2 frames.

This is useful to create landmarks and reduce the effect of speckle-noise for more robust feature detection and matching to find a fast with low computational expensive landmarks in the frame, which in turn depends on the orientation and the temperature profile of the baby.

D. Feature Point Detection and Matching

To classify and compare similarities between multiple thermal images, isolation of a set of distinct features between the images is required, e.g., edges, corners, or smooth regions with similar features like blobs and ridges.

Two category features can be extracted from an image, as mentioned in [8]:

• *Global Features:* The extracted features describe an image in such a way that images of similar nature can be detected. This is achieved by the classification of the properties of all the pixels in the image e.g., texture, colour histogram, etc. that are converted into a one multi-dimensional feature vector. However, the extracted features are not able to make a distinction between background and foreground.

• *Local Features:* The image is also represented based on its local structures and some of its salient features. These features include a set of local feature descriptors/vectors that are affine and scale-invariant. They are better suited for finding other occurrences of similar objects or regions of pixels in the images.

E. Contouring With Isotherms

The main process for tracking the ROI is contouring with isotherms. That is a normalized temperature-based segmentation of a frame into groups. The number of contour levels determines the threshold values for the grouping which results in polygons at each contour level. The encapsulated areas by the polygons in the frame represent the temperature values within the group level boundary. Considering the ROI related to an object (the baby) with the highest polygon temperature profile with the biggest area in the image is being selected to monitor the temperature.

F. Tracking the Detected Countour With Optical Flow

Douglas-Peucker (DP) algorithm [9] is used to reduce and simplify the number of connected data points during the creation of the Isotherm polygon. This Isotherm (ROI) is subjected to a tracking algorithm based on the Optical Flow (OF) algorithm. The reduced connected data points result in less number crunching and a faster tracking mechanism of the detected contour Fig. 6. However, the polygon's shape described by fewer data points becomes less accurate.

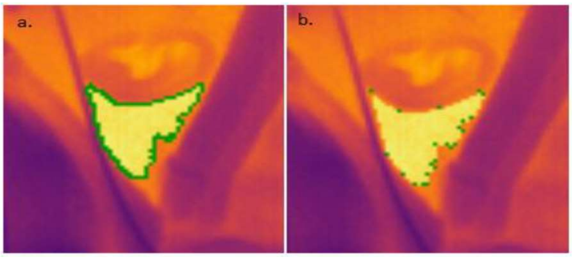

Fig. 6. (a) Detected original ROI (b) Same ROI using DP-algorithm. The calculated ROI areas (highlighted yellow color) in both (a) & (b) are equal.

Although, there is an optimum trade-off between the number of points describing the polygon and the polygon's deformation. Experiments show that the number of data points describing the ROI can be reduced by around 90% whilst the area of the polygon can vary by less than 10%.

G. Controur Level Noise Compensation (Region of Interest Deformation)

The tracking algorithm of isotherm contours could be unstable due to existing IR-camera thermal noise. A data normalization step can help to reduce this instability. Although, fluctuations in temperature readings and the elasticity of neonate's skin can stretch and deform the ROI shape considerably, which in turn influences the tracking process. The reason is that the ROI temperature values could show values below the contour level especially when these values are close to each other. As a result, the contouring algorithm will follow the next biggest sub-area of the ROI.

The influence of this error is solved by reducing the amount of noise in the contouring level threshold. For example, if the contouring level is set to be 10, the normalized data of the whole frame will be divided equally by 11 threshold points (0, 0.1, 0.2, ..., 0.9, 1). The highest threshold group with values 0.9 and 1 will be used to search for the ROI in the highest group. Consequently, the lower threshold of this group will be influenced and lowered by the value of the noise so that the new ranges become 0.9 mines noise to 1. Lowering the threshold may result in adding new areas which were not part of the initial detected ROI. But an overlapping step in the process will eliminate these areas.

Moreover, the calculated noise values are based on 3σ of the thermal noise of the IR-camera, that is 50mK as reported in [10]. The contour noise level compensation is thus normalized by the maximum and minimum from the data normalization which shows a very stable and accurate ROI area tracking.

H. External Disturbance Detection on Virtual Field of View

Tracking of the ROI always takes place inside the virtual FOV. In a parallel process, the next step of the tracking algorithm monitors disturbances along the boundaries of the virtual FOV.

It is possible that an external intervention like the hands of the care providers, other objects like blankets, or movements of the baby masquerade the FOV of the IR camera or that the ROI moves out of the virtual FOV (see Fig. 4). This is because there is always a distance between the IR camera and the ROI of the object shown as two possible scenarios of thermographic measurement models depicted in Fig. 2.

By defining the virtual FOV in the reference frame, a set of data points defines the green boundary as depicted in Fig. 4 (left). After receiving new frames from the IR camera, the algorithm creates a new virtual FOV on each frame and performs OF on the reference frame, and checks for disruptions in the frame.

Consequently, on receiving new frames from the IR camera the algorithm creates new virtual FOVs on each frame and it performs OF between the reference frame and new frame to check for any external intervention (disturbances) and compare them only for disruption along the boundary of the virtual FOV.

If there is any boundary disruption, the points in the boundary will be pushed outside the virtual FOV; as shown in Fig. 4 (right).

If the number of valid boundary points in the new frame is less than 80% of the reference boundary points, that particular frame is being discarded because there is a significant disturbance along the boundary of the virtual FOV. If no boundary disturbances are detected, then the algorithm continues with the tracking of the ROI.

IV. CONCLUSIONS

Our approach is a model-based, real-time algorithm that can detect and track a single thermographic profile in neonates, see Fig. 7. The algorithm can redetect partial of a reference TPR distorted by external interventions like hands of the care providers in the FOV or rapid movements of the neonates. This method is a robust and reliable technique for tracking the global and local ROI for short- and long-term (real-time up to 15 seconds, respectively). Moreover, simulations showed that reducing the number of frames per second (fps) from 9 to 1 fps will lower the number crunching but does not affect the TPR tracking.

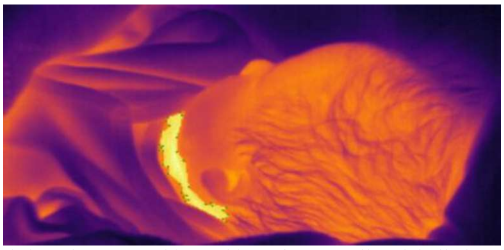

Fig. 7. Real-time thermographic tracking of RIO (yellow labelled area on the baby's neck).

ACKNOWLEDGMENTS

The authors would like to thank the parents of the neonates, hospital doctors, and nurses from the neonatology departments in South-Holland province in the Netherlands, and Erik Wirianto who gave support in doing experiments to gather results for this project. The outcome of this research is a group effort based on the European GDPR (General Data Protection Regulation) with the permission, collaboration, and dedication of these people.

REFERENCES

[1] Fluhr, J.W., et al. (2010). Functional skin adaptation in infancy - almost complete but not fully competent. Experimental Dermatology, 19(6), 483–492. https://doi.org/10.1111/j.1600-0625.2009.01023.x

[2] Martin, R. J., Miller, M. J., & Carlo, W. A. (1986). Pathogenesis of apnea in preterm infants. The Journal of Pediatrics, 109(5), 733–741. https://doi.org/10.1016/s0022-3476(86)80685-0

[3] Soll, R. F. (2008). Heat loss prevention in neonates. Journal of Perinatology, 28(S1), S57–S59. https://doi.org/10.1038/jp.2008.51

[4] Matej Kristan, et al.; The Seventh Visual Object Tracking VOT2019 Challenge Results, Proceedings of the IEEE/CVF International Conference on Computer Vision (ICCV), 2019, pp. 0-0.

[5] K. Rassels and P. French, "Accurate Body Temperature Measurement of a Neonate Using Thermography Technology," Smart System Integration (SSI) 2021 (online). DOI: 10.1109/SSI52265.2021.9467024

[6] A. F. Mills, Basic Heat and Mass Transfer, 2nd ed., Pearson New International Edition: Pearson Education Limited 2014, pp. 502.

[7] Rafael C. Gonzalez and Richard E. Woods. 2001. Digital Image Processing (2nd. ed.). Addison-Wesley Longman Publishing Co., Inc., USA.

[8] Awad, A. I. ve Hassaballah, M. (Ed.). (2016). Image Feature Detectors and Descriptors. Studies in Computational Intelligence. Springer International Publishing. doi:10.1007/978-3-319-28854-3

[9] Douglas, D. H., & Peucker, T. K. (1973). Algorithms for the Reduction of the Number of Points Required to Represent a Ditized Line or its Caricature. Cartographica: The International Journal for Geographic Information and Geovisualization, 10(2), 112–122. https://doi.org/10.3138/fm57-6770-u75u-7727.

[10] FLIR SC305 Datasheet. 2010 FLIR Systems.